

RECLAMATION

Managing Water in the West

Technical Report No. SRH-2014-30

Evaluating Climate-Induced Runoff and Temperature Change on Stream Habitat Metrics for Endangered or Threatened Fish



US Department of the Interior
Bureau of Reclamation
Technical Service Center

September 2014

Mission Statements

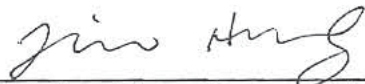
The Department of the Interior protects and manages the Nation's natural resources and cultural heritage; provides scientific and other information about those resources; and honors its trust responsibilities or special commitments to American Indians, Alaska Natives, and affiliated island communities.

The mission of the Bureau of Reclamation is to manage, develop, and protect water and related resources in an environmentally and economically sound manner in the interest of the American public.

Technical Report No. SRH-2014-30

Evaluating Climate-Induced Runoff and Temperature Change on Stream Habitat Metrics for Endangered or Threatened Fish

Prepared by:



Jianchun Victor Huang, Ph.D., P.E.
Hydraulic Engineer
Sedimentation and River Hydraulics Group, 86-68240

9/30/2014

Date

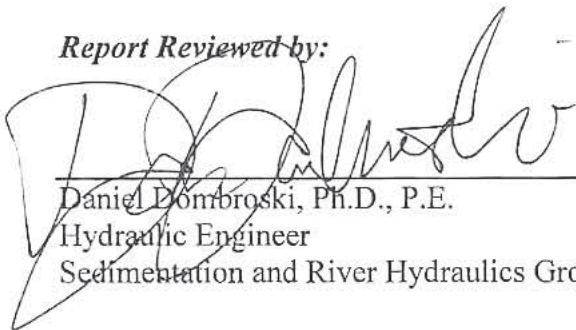


Jennifer Bountry, M.S., P.E.
Hydraulic Engineer
Sedimentation and River Hydraulics Group, 86-68240

9/30/2014

Date

Report Reviewed by:



Daniel Dombroski, Ph.D., P.E.
Hydraulic Engineer
Sedimentation and River Hydraulics Group, 86-68240

9/30/14

Date

Table of Contents

| | |
|---|------------|
| TABLE OF CONTENTS | I |
| LIST OF FIGURES | II |
| LIST OF TABLES | III |
| EXECUTIVE SUMMARY | V |
| 1. INTRODUCTION..... | 1 |
| 2. TEMPERATURE MODEL | 1 |
| 2.1 TEMPERATURE EQUATION..... | 2 |
| 2.2 SOLAR RADIATION | 2 |
| 2.3 ATMOSPHERE RADIATION..... | 5 |
| 2.4 OUTGOING BLACK-BODY RADIATION..... | 6 |
| 2.5 EVAPORATIVE HEAT LOSS..... | 6 |
| 2.6 CONDUCTION HEAT LOSS TO AIR..... | 6 |
| 2.7 HEAT EXCHANGE WITH STREAM BED..... | 7 |
| 3. METHOW RIVER TEMPERATURE MODELING..... | 7 |
| 3.1 TEST CASE WITH FLIR DATA..... | 9 |
| 3.2 TEST CASE WITH LOG DATA..... | 14 |
| 4. CLIMATE CHANGE IMPACT ON THE TEMPERATURE OF THE METHOW RIVER..... | 18 |
| 5. CONCLUSIONS | 23 |
| 6. RECOMMENDATIONS..... | 24 |
| ACKNOWLEDGMENTS | 25 |
| REFERENCES..... | 25 |

LIST OF FIGURES

| | |
|--|----|
| Figure 3-1. Site map of the Methow River, WA..... | 8 |
| Figure 3-2. TIR imagery taken on August 26 2009 in the vicinity of the Chewuch River and Spring Creek. The color scale is mapped to measured water surface temperature. Warmer water from Chewuch River enters on the river left and colder water from the Spring Creek enters on the river right. Flow direction is from left to right. | 10 |
| Figure 3-3. SRH-2D numerical simulation of water temperature at the confluences with the Chewuch River and the Spring Creek, with tributaries modeled as point sources. Color scale is mapped to predicted depth-averaged temperature. Flow direction is from left to right. | 11 |
| Figure 3-4. SRH-2D numerical simulation of water temperature at the confluences with the Chewuch River and the Spring Creek, with the Spring Creek contribution modeled as a combination of point-source and non-point source seeps from the right bank. Color scale is mapped to predicted depth-averaged temperature. | 12 |
| Figure 3-5. SRH-2D numerical simulation of water temperature at the confluences with the Chewuch River and the Spring Creek, modeled with an order of magnitude reduction in the turbulent Prandtl number. Reduction in the turbulent Prandtl number decreases the persistence of temperature gradients downstream of the tributary confluences. | 13 |
| Figure 3-6. SRH-2D numerical simulation of water temperature at the confluences with the Chewuch River and the Spring Creek, modeled with an order of magnitude increase in the turbulent Prandtl number. Increasing the turbulent Prandtl number increases the persistence of temperature gradients downstream of the tributary confluences. | 14 |
| Figure 3-7. Temperature loggers located in the study reach..... | 15 |
| Figure 3-8. Methow and Chewuch hydrographs used as upstream input boundary conditions. | 16 |
| Figure 3-9. Methow, Chewuch, and Spring Creek inflow water temperatures used as upstream input boundary conditions for the model. | 17 |
| Figure 3-10. Measured and simulated water temperatures at the logger location labeled Methow above Barkley Diversion. | 18 |
| Figure 4-1. Plots of the summer temperature and flow for each historical and future period. Colored triangles indicate the scenario pair selected that is described more fully in Table 4-1. This current study demonstrates how SRH-2D model could be used to predict the water temperature under climate change impact along the rivers where the flow and temperature are only available from simplified VIC simulation and statistical analysis at upstream gage stations. A temperature distribution can be provided by SRH-2D under climate change. Simulated temperatures at the US 20 bridge crossing in Winthrop are presented in Figure 4-2 to Figure 4-4, which could be used to provide information in reaches utilized by endangered or threatened fish species. | 20 |
| Figure 4-2 Simulated summer water temperature at the US 20 bridge crossing in Winthrop in hot and dry scenario. | 21 |
| Figure 4-3 Simulated summer water temperature at the US 20 bridge crossing in Winthrop in median scenario. | 21 |
| Figure 4-4 Simulated summer water temperature at the US 20 bridge crossing in Winthrop in cool and wet scenario. | 22 |

Figure 4-5. Average summer temperature for each historical and future period. Blue represents input temperature at upstream Methow River; red represents input temperature at upstream Chewuch River, and green represents the simulated water temperature at downstream of Methow at Winthrop at the US 20 bridge crossing in Winthrop.23

LIST OF TABLES

| | |
|--|----|
| Table 2-1. Coefficients of solar radiation reflection. | 3 |
| Table 2-2 Coefficients a_3 and b_3 describing the reflection of solar radiation at the water surface (source: Martin and McCutcheon, 1999; and Marciano and Harbeck, 1954)..... | 5 |
| Table 2-3. Coefficients to compute saturation vapor pressure..... | 6 |
| Table 3-1 Incoming flow rates and temperatures..... | 9 |
| Table 3-2 Logger data available in the study reach. | 15 |
| Table 4-1. Details of the models picked, reference vectors, and selected values of temperature and flow for each scenario, historical and future period. Relative year indicates the summer within the 1916-2006 sample for each 91-year time series. | 19 |

Executive Summary

This research aims to develop and assess a methodology to estimate the impact of climate change on stream temperature. Specifically, the research is aimed to study how climate change will alter water temperature inputs to stream and floodplain reaches utilized by endangered or threatened fish species. The temperature module was developed in the Sedimentation and River Hydraulic for an existing 2D hydraulic and sediment transport model, SRH-2D. The SRH-2D temperature model utilizes meteorological data as inputs (solar radiation, cloud cover, air temperature, dew point temperature, and wind speed). Physical processes include solar radiation, terrain and vegetation shade, atmospheric radiation, water back radiation, heat exchange between water and river bed, water surface evaporative and conductive losses. While there are opportunities for continued improvements and testing due to the complexity of input variables and calibration parameters, the temperature module is operational and able to be applied to engineering problems and climate change questions.

In this study, the temperature module in SRH-2D was first debugged and verified in a reach of the Methow River near Winthrop, WA since it had not previously been applied to an engineering problem. The Methow River reach has a warmer water tributary entering on river left and colder water springs entering from river right. Test one involved using FLIR data that represents a grid of surface temperatures at a single river flow and a single point in time. This data was used to test how well the model can represent lateral changes in temperature across the channel. Surface water temperature can be different than depth-averaged temperature, which is computed by the 2D model. This difference may cause some variance in how well the 2D model results can represent the FLIR data, particularly in areas where the mixing rate of the river is slow or highly variable. However, the Methow is generally well mixed due to a steep slope and fairly shallow depths. Test two used three loggers that provide continuous data over several months from spring to fall. The loggers provided a test of how well the model could represent temporal changes in temperature. After the model was tested with historical data, SRH-2D was also used to study how climate change will alter water temperature in the Methow River.

The model showed good accuracy in simulating the lateral temperature mixing zones downstream of tributary confluences when the model is well calibrated by adjusting the Prandtl number. The Prandtl number represents the ratio between the temperature diffusion and momentum diffusion coefficients. It was also shown that non-point source boundary conditions may be required to model spatially distributed contributions such as seepage of cold water from a spring.

The model was generally successful in reproducing the measured temporal variation in temperature measured. In this four mile test reach, the water temperature is mostly driven by incoming flow discharge and temperature, and not sensitive to weather/climate. For the Methow River, it is hypothesized from measured data that weather impacts to water temperature occur on the scale of multiple reaches, perhaps on the order of tens of river miles. This may not hold true on other river reaches with longer flow residence times.

The climate change impact on the stream temperature was successfully demonstrated in hot-dry, cool-wet, and median scenarios. We found that over a typical river reach of a few miles, the influence of meteorology on water temperature predictions was minimal. Over a reach scale, water temperature predictions were mainly controlled by the incoming water temperature and localized inputs such as the warmer tributary and colder springs. The vast amount of climate change data at an hourly scale posed computational limitations with running the 2D model.

1. Introduction

Climate change is a long-term shift in the weather of a region, which may include temperature, precipitation, wind, or other factors. Climate change usually occurs when there are changes in the earth's absorption of the sun's energy, circulation of the ocean and atmosphere, and/or emission of energy into space over an extended period of time. Recently, much attention has been paid to the impact of climate change on water supply such as the timing and magnitude of flows (e.g., Brekke et al., 2010; Vicuna and Dracup, 2007; Miller et al., 2003). Little is known about the effects of climate change on river water temperature.

This research aims to develop and assess a methodology to estimate the impact of climate change on stream temperature. Specifically, the research is aimed to study how climate change will alter water temperature inputs to stream and floodplain reaches utilized by endangered or threatened fish species. Stream temperature is critical to the health and productivity of aquatic ecosystems (Caissie, 2006; Webb et al., 2008; and Caldwell et al., 2013). Climate change may impact temperature patterns in the Pacific West. Higher summer water temperatures may directly affect salmonids in each life stage, whether egg, fry, fingerling, smolt, or adult. It may also affect the fish indirectly through effects on other environmental factors such as food supplies, diseases, dissolved oxygen, and increased predation (Boles, 1988).

Lai and Mooney (2009) developed a two-dimensional (2D) temperature module for an existing 2D hydraulic and sediment transport model, SRH-2D. The 2D model incorporates data with both lateral and longitudinal geographic extents rather than lumping results into a point-to-point or uni-directional representation. The improved representation of spatial features allows more accurate simulation of lateral changes in temperature across the channel. The SRH-2D temperature model utilizes meteorological data as inputs (solar radiation, cloud cover, air temperature, dew point temperature and wind speed). Physical processes modeled include solar radiation, terrain and vegetation shade, atmospheric radiation, water back radiation, heat exchange between water and river bed, water surface evaporative and conductive losses.

In this research, the SRH-2D temperature model was verified in a reach of the Methow River near Winthrop, WA. The Methow River reach has a warmer water tributary entering on river left and a colder water spring entering from river right. Two sets of data were used to test the model. Test one involved using FLIR data that represents a grid of surface temperatures at a single river flow and a single point in time. This data was used to test how well the model can represent lateral changes in temperature across the channel. Surface water temperature can be different than depth-averaged temperature, which is computed by the 2D model. This difference may cause some variance in how well the 2D model results can represent the FLIR data, particularly in areas where the mixing rate of the river is slow or highly variable. However, the Methow is generally well mixed due to a steep slope and fairly shallow depths. Test two used three loggers that provide continuous data over several months from spring to fall. The loggers provided a test of how well the model could represent longitudinal changes in temperature. SRH-2D was also used to study how climate change will alter water temperature in the Methow River.

2. Temperature Model

For better understanding of all terminologies in the temperature model, the temperature governing equation and its source terms are presented here. Most of these sections are from Lai and Mooney (2009).

2.1 Temperature Equation

The 2D depth-averaged flow equations are based on the assumptions that stream flows are shallow compared to width and the effect of vertical motion is negligible.

Conservation of thermal energy leads to the 2D depth-averaged temperature equation expressed as:

$$\frac{\partial hT}{\partial t} + \frac{\partial hUT}{\partial x} + \frac{\partial hVT}{\partial y} = \frac{\partial}{\partial x} \left[\frac{hv_t}{\sigma_t} \frac{\partial T}{\partial x} \right] + \frac{\partial}{\partial y} \left[\frac{hv_t}{\sigma_t} \frac{\partial T}{\partial y} \right] + \frac{\Phi_{net}}{c_w \rho_w} + \frac{q_{sp}}{A_{sp}} (T_{sp} - T) \quad (2.1)$$

In the above, T is depth averaged water temperature [C], x and y are horizontal Cartesian coordinates [m], t is time [s], h is water depth [m], U and V are depth-averaged velocity components [m/s] in x and y directions, respectively, v_t is the turbulent viscosity and dispersion [m²/s], σ_t is the turbulent Prandtl number, ρ_w is the water density [kg/m³], c_w is the specific heat of water [J/kg/C], q_{sp} is the spring water flow rate [m³/s] into the stream (zero if spring flows out), A_{sp} is the area [m²] of the spring water inflow, T_{sp} is the spring water temperature [C], and Φ_{net} is the net heat exchange [w/m²] between water column and its surroundings (through water surface and streambed). The turbulent eddy viscosity (v_t) is computed with a turbulence model (Rodi, 1993).

The net heat flux, Φ_{net} , consists of six contributions as follows:

$$\Phi_{net} = \Phi_{ns} + \Phi_{na} + \Phi_{bed} - \Phi_{br} - \Phi_e - \Phi_c \quad (2.2)$$

where

Φ_{ns} = net solar radiation entering water surface;

Φ_{na} = net atmospheric radiation entering water surface;

Φ_{br} = heat loss by back radiation from stream (black body radiation);

Φ_e = evaporative heat loss at water surface;

Φ_c = conductive heat loss at water surface; and

Φ_{bed} = heat flux into stream at channel bed.

The net solar radiation at a water surface incorporates five thermal processes: extra-terrestrial solar radiation, attenuation due to atmosphere, correction for cloud cover, reflection by water surface, and correction due to terrain and vegetation shade. The processes are described fully in a number of reports and textbooks on hydrology (e.g., Huber and Harleman, 1968; Eagleson, 1970; and Brutsaert, 1991).

2.2 Solar Radiation

If measured solar radiation (Φ_{sm}) at water surface is available, the net solar radiation is computed as (Hauser and Schohl, 2003)

$$\Phi_{ns} = \Phi_{sm} R_s \quad (2.3)$$

where Φ_{sm} is measured solar radiation (shade free solar radiation at the water) and R_s is reflection and terrain and vegetation shading factor which is computed by the following equations (Hauser and Schohl, 2003):

$$R_s = \begin{cases} R_{sm} & \text{if } X_n \leq B \text{ (shade free)} \\ 0.2 & \text{if } X_n > B + W \text{ (full shade)} \\ R_{sm} \frac{B+W-X_n}{W} + 0.2 \frac{X_n-B}{W} & \text{if } B < X_n \leq B + W \text{ (partial shade)} \end{cases} \quad (2.4)$$

In the above:

$R_{sm} = 1 - a(57.3\alpha)^{-b}$ = shade-free reflection factor (a and b see Table 2-1);

α = solar altitude in radians;

W = width of the stream cross section;

B = distance from trees to water edge;

$X_n = H_b \cos \beta / \tan \alpha$ = normal distance from trees to shadow edge;

H_b = tree and bank height from water surface;

$\beta = |\theta - 90/57.3|$ = angle between sun and stream axis normal in radian;

$\theta = \left| A_{zs} - \frac{A_{zr}}{57.3} \right|$ = angle between sun and stream axis in radian;

A_{zr} = river azimuth, clockwise from north to direction of flow in degree;

A_{zs} = sun azimuth in radian calculated by $\cos A_{zs} = -\frac{\sin \phi \sin \alpha - \sin \delta}{\cos \phi \cos \alpha}$.

ϕ = site latitude in radians; and

δ = is sun declination (between the sun and equator) in radians.

Table 2-1. Coefficients of solar radiation reflection.

| Cloud Cover C | a | b |
|-----------------|------|------|
| 0-0.05 | 1.18 | 0.77 |
| 0.05 – 0.5 | 2.20 | 0.97 |
| 0.5 – 0.92 | 0.95 | 0.75 |
| 0.92 – 1.0 | 0.35 | 0.45 |

The solar altitude α is computed assuming spherical geometry, as follows (Huber and Harleman, 1968):

$$\sin \alpha = \sin \phi \sin \delta + \cos \phi \cos \delta \cos h \quad (2.5)$$

where ϕ is site latitude in radians, δ is sun declination in radians, and h is the sun hour angle in radians.

If no measured solar radiation (Φ_{sm}) is available, the solar radiation that reaches the water surface can be estimated from (Martin and McCutcheon, 1999)

$$\Phi_{sm} = H_0 a_t C_a \quad (2.6)$$

where H_0 = the amount of radiation reaching the earth's outer atmosphere (Wm^{-2}); a_t = radiation scattering and absorption factor; C_a = the fraction of solar radiation not absorbed by clouds.

The fraction of solar radiation passing through the clouds is given by the cloud cover (C) as

$$C_a = 1 - 0.65C^2 \quad (2.7)$$

The flux of solar radiation that strikes the earth's outer atmosphere is estimated from

$$H_0 = \frac{H_{sc}}{r^2} \left[\sin\phi \sin\delta + \frac{12}{\pi} \cos\phi \cos\delta (\sin h_e - \sin h_b) \right] \Gamma \quad (2.8)$$

where H_{sc} = the solar constant (1390 Wm⁻²); r = the relative distance (-) between the earth and sun; ϕ = the site latitude in radians; δ = sun declination (between the sun and equator) in radians; h_e and h_b = the solar hour angles at the end and the beginning of the time period over which H_0 is being calculated, respectively; and Γ = a correction factor for diurnal exposure to the radiation flux. The relative earth-sun distance can be estimated from

$$r = 1.0 + 0.017 \cos \left[\frac{2\pi}{365} (186 - D_y) \right] \quad (2.9)$$

where D_y = the Julian day of the year. The declination of the sun can be estimated from

$$\delta = \frac{23.45\pi}{180} \cos \left[\frac{2\pi}{365} (172 - D_y) \right] \quad (2.10)$$

The hour angles (radians) at the beginning and ending of the period over which H_0 is being calculated is computed from

$$h_b = \left\{ \frac{\pi}{12} [(h_r - 1) - \Delta t_s + 12a_2] \right\} + b_2(2\pi) \quad (2.11)$$

$$h_e = \left\{ \frac{\pi}{12} [h_r - \Delta t_s + 12a_2] \right\} + b_2(2\pi) \quad (2.12)$$

where h_r is the hour of the day from 1 to 24; the coefficient $a_2 = 1.0$ for $h_r \leq 12$ and $a_2 = -1.0$ for $h_r > 12$. The coefficient b_2 varies with the magnitude of the quantity inside the curly brackets for both h_b and h_e in Eqs. (2.11) and (2.12). The coefficient $b_2 = -1$ for $\{\cdot\} > 2\pi$, $b_2 = 1$ for $\{\cdot\} < 0$, and $b_2 = 0$ otherwise.

The fraction of an hour between the standard meridian and the local meridian is Δt_s . In the United States, the standard meridians are at 75°, 90°, 105°, and 120° for eastern, central, mountain, and Pacific Time zones; respectively. The fraction can be calculated from

$$\Delta t_s = \frac{E_a}{15} (L_{sm} - L_{lm}) \quad (2.13)$$

where L_{sm} is the standard meridian, L_{lm} is the local meridian. $E_a = -1$ for west longitude and $E_a = 1$ for east longitude. For example, at Methow River at Winthrop, $L_{sm} = 120^\circ$ (Pacific Time zone), $L_{lm} = 120.167639^\circ$ (longitude of Winthrop), and $E_a = -1$ for west longitude.

The correction factor Γ in Eq.(2.8) is set to one at day time (between sunrise and sunset) and zero at night time. The standard time of sunset and sunrise can be estimated from

$$t_{ss} = \frac{12}{\pi} \cos^{-1} \left(-\frac{\sin\phi\sin\delta}{\cos\phi\cos\delta} \right) + \Delta t_s + 12 \quad (2.14)$$

$$t_{su} = -t_{ss} + 2\Delta t_s + 24 \quad (2.15)$$

The radiation scattering and absorption factor a_t in Eq.(2.6) can be estimated from

$$a_t = \frac{t+0.5(1-s-c_d)}{1-0.5R_g(1-s-c_d)} \quad (2.16)$$

where c_d is a dust coefficient, which has a range of 0.0 to 0.13 and a typical value of 0.06; and R_g is the reflectivity of the water surface, which varies with the type of cloud cover as

$$R_g = a_3 \left(\frac{180}{\pi} \alpha \right)^{b_3} \quad (2.17)$$

where α is the solar altitude in radians, calculated in Eq.(2.5) and a_3 and b_3 are coefficients (Table 2-2) depending on the cloud cover (C).

Table 2-2 Coefficients a_3 and b_3 describing the reflection of solar radiation at the water surface (source: Martin and McCutcheon, 1999; and Marciano and Harbeck, 1954).

| Description | Fraction Cloud Cover (C) | a_3 | b_3 |
|-------------|--------------------------|-------|-------|
| Overcast | $C > 0.9$ | 0.33 | -0.45 |
| Broken | $0.5 < C < 0.9$ | 0.95 | -0.75 |
| Scattered | $0.1 < C < 0.5$ | 0.5 | -0.97 |
| Clear | $C < 0.1$ | 1.18 | -0.77 |

The mean atmospheric transmission coefficient s and t in Eq. (2.16) is given by

$$s = \exp[-(0.465 + 0.134P_{wc})(0.129 + 0.171 \exp(-0.88\theta_{am}))\theta_{am}] \quad (2.18)$$

$$t = \exp[-(0.465 + 0.134P_{wc})(0.179 + 0.421 \exp(-0.721\theta_{am}))\theta_{am}] \quad (2.19)$$

where θ_{am} is the dimensionless optical mass, P_{wc} is the mean daily precipitable atmospheric water content, given by

$$P_{wc} = 0.85 \exp(0.11 + 0.0614T_d) \quad (2.20)$$

$$\theta_{am} = \left(\frac{288 - 0.0065Z}{288} \right)^{5.256} / \left[\sin \alpha + 0.15 \left(\frac{180\alpha}{\pi} + 3.855 \right)^{-1.253} \right] \quad (2.21)$$

where T_d = the dewpoint temperature [C], Z = the site elevation (m) and α = the solar altitude in radians, calculated in Eq.(2.5).

2.3 Atmosphere Radiation

The net long-wave radiation (atmospheric radiation entering water surface) is computed as:

$$\Phi_{na} = 5.16432 \cdot 10^{-13} (1 + 0.17C^2)(T_a + 273.16)^6 \quad (2.22)$$

where C is cloud cover, fraction of the sky covered by clouds, and T_a is dry bulb air temperature [C].

2.4 Outgoing Black-Body Radiation

The outgoing black-body radiation emitted from the water surface is a function only of the water temperature, and it is given by (Huber and Harleman, 1968):

$$\Phi_{br} = \varepsilon_w \sigma (T_w + 273.16)^4 \quad (2.23)$$

where T_w is water-surface temperature [C], ε_w is emissivity (0.97 by Huber and Harleman (1968) and 0.98 by Tung et al. (2006), and σ is Stefan-Boltzman constant ($5.672 \times 10^{-8} \text{ w/m}^2/\text{K}^4$). In the current model, the depth averaged temperature T is used for T_w .

2.5 Evaporative Heat Loss

The evaporative heat loss is computed by:

$$\Phi_e = \rho_w L (a_1 + b_1 W_a) (e_s - e_a) \quad (2.24)$$

where:

$L = 4184(597 - 0.57T_w)$ = the latent heat [J/kg];

T_w = water surface temperature in Celsius;

W_a = wind speed (m/s);

a_1, b_1 = constants: $a_1 = 0.0$ to $4.0\text{e-}9$; $b_1 = 1.0\text{e-}9$ to $3.0\text{e-}9$;

$e_a = 2.171 \times 10^8 \exp\left[-\frac{4157}{T_d + 239.09}\right]$ = saturation vapor pressure [mb];

T_d = dewpoint temperature in Celsius; and

$e_s = \alpha_j + \beta_j T_w$ = saturation vapor pressure [mb] with coefficients in Table 2-3

Table 2-3. Coefficients to compute saturation vapor pressure.

| T | j | α_j | β_j |
|-------|---|------------|-----------|
| 0-5 | 1 | 6.05 | 0.522 |
| 5-10 | 2 | 5.10 | 0.710 |
| 10-15 | 3 | 2.65 | 0.954 |
| 15-20 | 4 | -2.04 | 1.265 |
| 20-25 | 5 | -9.94 | 1.659 |
| 25-30 | 6 | -22.29 | 2.151 |
| 30-35 | 7 | -40.63 | 2.761 |
| 35-40 | 8 | -66.90 | 3.511 |

2.6 Conduction Heat Loss to Air

The conduction heat loss is:

$$\Phi_c = 0.61 \times 10^{-3} \rho_w L (a_1 + b_1 W_a) P (T_w - T_a) \quad (2.25)$$

where P is air barometric pressure [mb] and a_1 and b_1 are defined the same as in Eq.(2.24), T_w is water surface temperature [C], and T_a is dry bulb air temperature [C].

2.7 Heat Exchange with Stream Bed

Heat exchange between stream bed and stream water is significant for shallow streams and it consists of two contributions: conduction from bed to stream and net solar radiation entering bed. It is computed by the following expression:

$$\Phi_{bed} = \frac{k_b}{0.5\delta_b} (T_b - T_w) - (1 - A_b)(1 - \beta) \exp[-\eta(D - 0.6)] \Phi_{ns} \quad (2.26)$$

where k_b is the thermal conductivity of the streambed bed material, δ_b is the effective bed thickness used for heat conduction computation, T_w is the water temperature, T_b is the effective stream bed temperature which is updated each time step by $T_b = T_b^{old} - \frac{\Phi_{bed}\Delta t}{\rho_b C_b \delta_b}$ with ρ_b and C_b the density and specific heat of the bed materials and Δt is the time step for simulation, A_b is albedo of bed material, β is fraction of solar radiation absorbed in the top 0.6m of surface water, η is extinction coefficient in water [1/m], and D is water depth [m].

3. Methow River Temperature Modeling

The SRH-2D temperature model is verified in a reach of the Methow River near Winthrop, WA (Figure 3-1). The Methow River is a tributary of the Columbia River in northern Washington State. The river's watershed is 1,890 square miles (4,900 km²). Much of the river basin is located in national forests and wildernesses. The Methow River and its tributaries historically support prolific runs of Chinook and Coho Salmon, summer steelhead, and other native fishes. However, these native fish populations have experienced substantial declines from their historical numbers. Reclamation is completing studies that will create better in-stream and riparian habitat for salmon and steelhead. To understand the habitat quality, stream temperature is being studied, including effects of projected climate change.

The four mile reach of the Methow River near Winthrop, WA is chosen to study the impact of climate change on the river temperature. In the study reach, there is a warm water tributary (the Chewuch River) entering on the river left and a cold water spring (the Spring Creek) entering on the river right. Due to the steep slope and fairly shallow depths, the Methow is generally well-mixed. The comparison between surface radiant temperature derived from the TIR images and in-stream monitors is usually within 0.2°C with a target accuracy of 0.5°C (Watershed Sciences, 2009). Thus magnitude of temperature gradient in the vertical direction is usually within 0.2 degree. A depth-averaged model, such as SRH-2D, is appropriate for this reach-based application. Localized areas of vertical differentiation in water temperature may occur where groundwater inputs to the stream, deep bedrock pools persist, or warm water irrigation returns to the main channel.

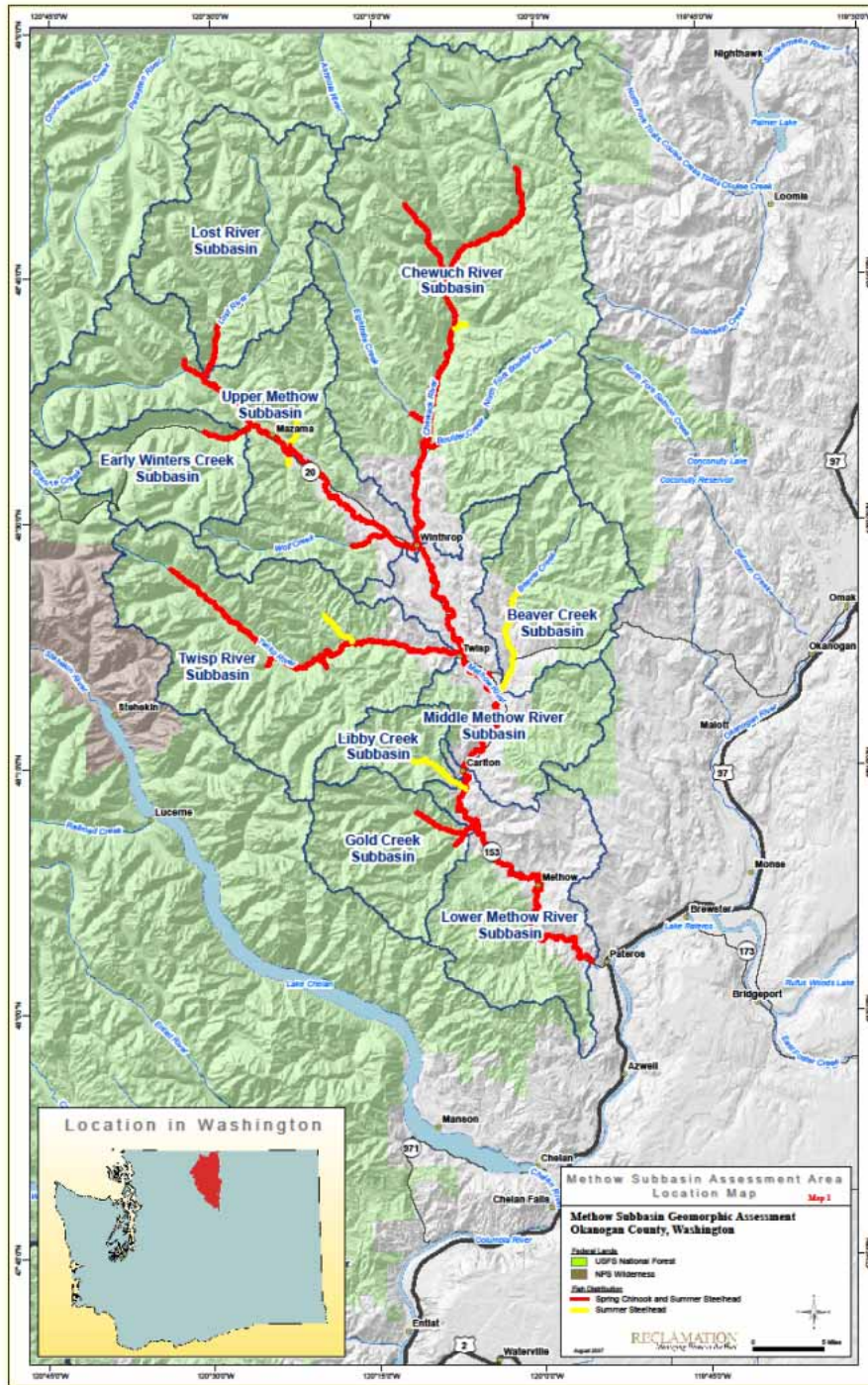


Figure 3-1. Site map of the Methow River, WA.

Two types of temperature data collected in the Methow River were used to test the SRH-2D temperature model. The first test case involves using FLIR data that represents a grid of surface temperatures at a single river flow and a single point in time. Images were collected with a FLIR system’s SC6000 sensor (8-9.2 m) mounted on the underside of a Bell Jet Ranger Helicopter. This

data is used to test how well the model can represent lateral changes in temperature across the channel. No heat source terms were used in this case.

In the second case, the model is tested with 3 loggers that provide continuous data over several months. The loggers provide a test of how well the model can represent longitudinal changes in temperature. The heat sources, including the solar and atmospheric radiations entering water surface, evaporative heat loss, et al. were calculated and some of the terms were calibrated.

3.1 Test Case with FLIR Data

Watershed Sciences (2009) provided thermal infrared (TIR) remote sensing imagery for approximately 160 river miles in the Methow River Basin for the Yakama Tribe Fisheries. TIR images were collected with a FLIR system’s SC6000 sensor mounted on the underside of a helicopter. Airborne TIR was used to map spatial temperature patterns in the Methow River. TIR images were recorded during a three-day flight from August 24 to August 26, 2009 over the Methow, Twisp, and Chewuch Rivers. A four mile reach of the Methow River near Winthrop is used to simulate the two-dimensional temperature dynamics downstream of the Chewuch River Spring Creek confluences.

Simulated 2D water temperature is compared to measured surface temperature to test the ability of the model in predicting lateral thermal mixing. Surface water temperature (measured) may be different than depth-averaged temperature (computed) due to stratification. This difference may cause some variance in how well the 2D model results can represent the TIR data, particularly in areas where the mixing rate of the river is slow or highly variable. The Methow is, however, generally well-mixed due to a steep slope and fairly shallow depths. For this reason, the surface water temperature is used for the model upstream boundary condition.

Two river gage stations are located in the study reach, USGS 12448500 (Methow at Winthrop downstream of the confluence of the Methow and Chewuch) and USGS 12448000 (Chewuch at Winthrop upstream of the confluence). On August 26, 2009, the flow rate of Methow at Winthrop was 275 cfs and that of Chewuch at Winthrop was 89.1 cfs. The combined flow in the Methow River and Spring Creek above the Chewuch -is obtained from the difference between the two gages. Then, the incoming discharge for Spring Creek and the Methow River was solved by assuming the incoming temperature and discharge product for each tributary equals the temperature and discharge product in the downstream river at the gage. The flow rates at the Methow River above the Chewuch is set as 146.0 cfs and the combined flows from Spring Creek is set as 40.8 cfs., to reach a mixed temperature downstream of the Spring Creek 15.8 °C from the surveyed data. The calculation assumed that there is no heat sources and sinks within this short reach.

Table 3-1 Incoming flow rates and temperatures.

| | Flow Rate (cfs) | Temperature (°C) |
|--------------|-----------------|------------------|
| Chewuch | 89.1 | 17.3 |
| Methow | 146.0 | 15.4 |
| Spring Creek | 40.8 | 13.6 |

Figure 3-2 through Figure 3-4 display measured water surface temperature and simulated water temperature results. Figure 3-2 shows measured water surface temperature in the vicinity of the

Chewuch and Spring Creek confluences. The field data indicates the presence of temperature mixing zones downstream of the tributary confluences; the comparatively small inflow from Spring Creek produces a low temperature zone that is highly persistent in the streamwise direction, suggesting non-point source seepage along the bank. Figure 3-3 shows the SRH-2D simulated temperature using point-based model contributions from the Chewuch and Spring Creek. The simulation results qualitatively reproduce the zone of lateral temperature stratification downstream of the Chewuch, however vastly underpredict the extent to which the cold temperature zone persists downstream of Spring Creek.

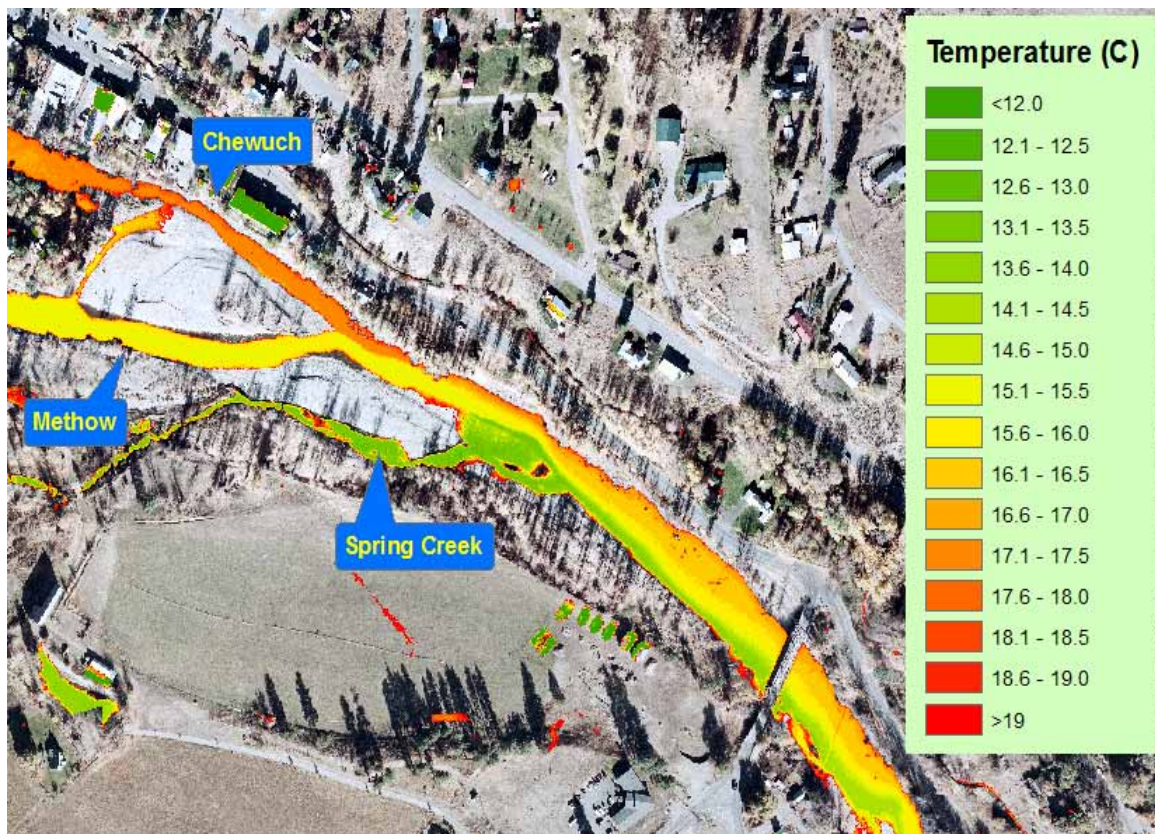


Figure 3-2. TIR imagery taken on August 26 2009 in the vicinity of the Chewuch River and Spring Creek. The color scale is mapped to measured water surface temperature. Warmer water from Chewuch River enters on the river left and colder water from the Spring Creek enters on the river right. Flow direction is from left to right.

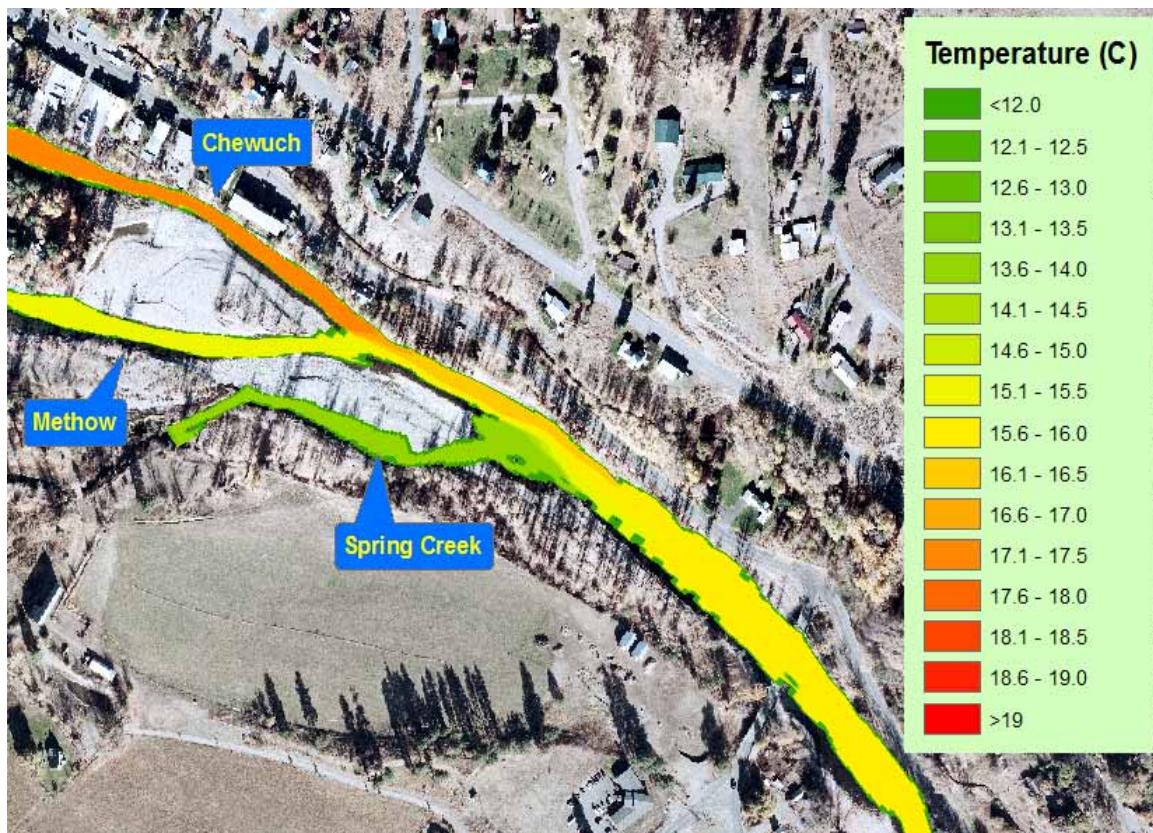


Figure 3-3. SRH-2D numerical simulation of water temperature at the confluences with the Chewuch River and the Spring Creek, with tributaries modeled as point sources. Color scale is mapped to predicted depth-averaged temperature. Flow direction is from left to right.

Figure 3-4 shows the SRH-2D numerical temperature simulation with a non-point source of water seeping into the stream from Spring Creek. From the calibration process, it was determined that a combination of 20.7 cfs modeled as point source from Spring Creek and 20 cfs modeled as non-point source seeps produces qualitative agreement with the measurements (Figure 3-2), predicting mixing zones from both tributaries fairly well.

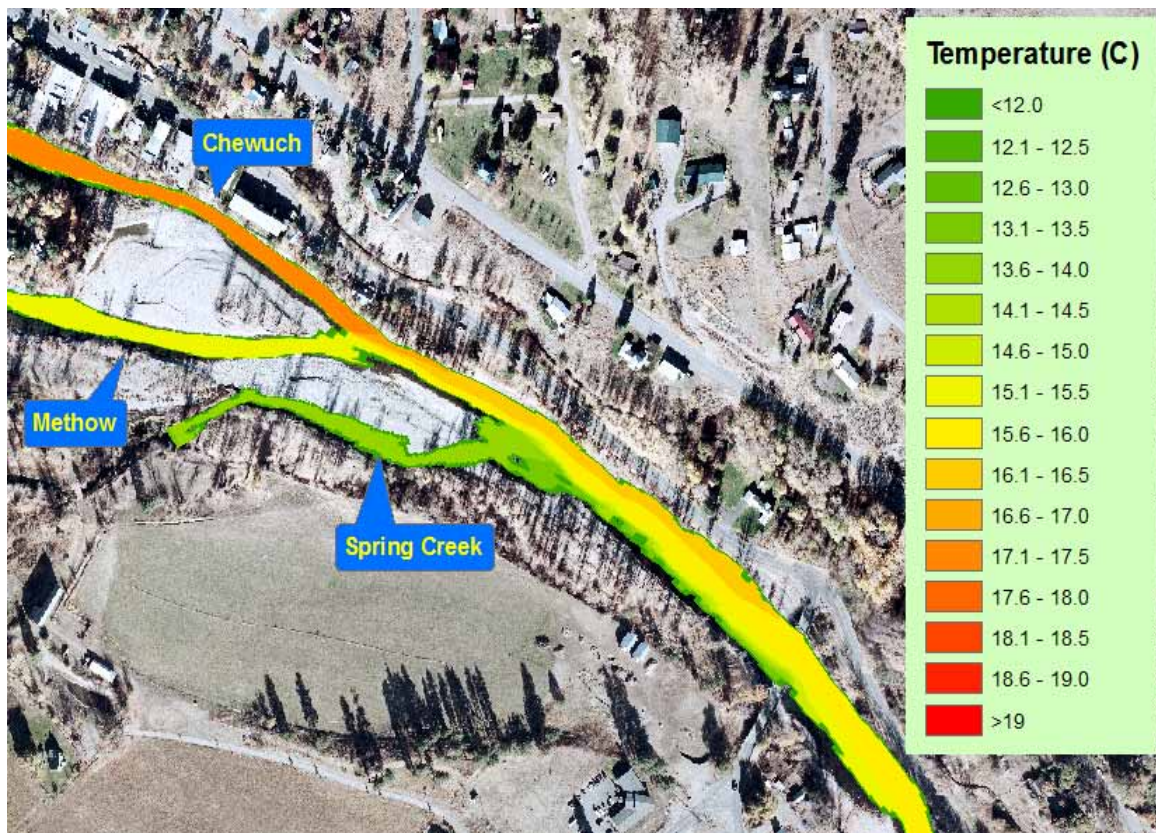


Figure 3-4. SRH-2D numerical simulation of water temperature at the confluences with the Chewuch River and the Spring Creek, with the Spring Creek contribution modeled as a combination of point-source and non-point source seeps from the right bank. Color scale is mapped to predicted depth-averaged temperature.

A sensitivity analysis was performed on the turbulent Prandtl number σ_t in Eq. (2.1). The turbulent Prandtl number is the ratio of momentum eddy diffusivity ν_t to thermal eddy diffusivity, and is typically on the order of one in natural turbulent flows. In the case of $\sigma_t > 1$, momentum diffusivity is greater than thermal diffusivity and therefore thermal gradients persist longer than momentum gradients. Figure 3-4 shows temperature simulation results modeled with a turbulent Prandtl number equal to unity. Figure 3-5 and Figure 3-6 show temperature simulation results modeled with an order of magnitude decrease (0.1) and an order of magnitude increase (10), respectively, in the turbulent Prandtl number. The results show that decreasing (increasing) the turbulent Prandtl number decreases (enlarges) the persistence of temperature gradients downstream of the tributary confluences.

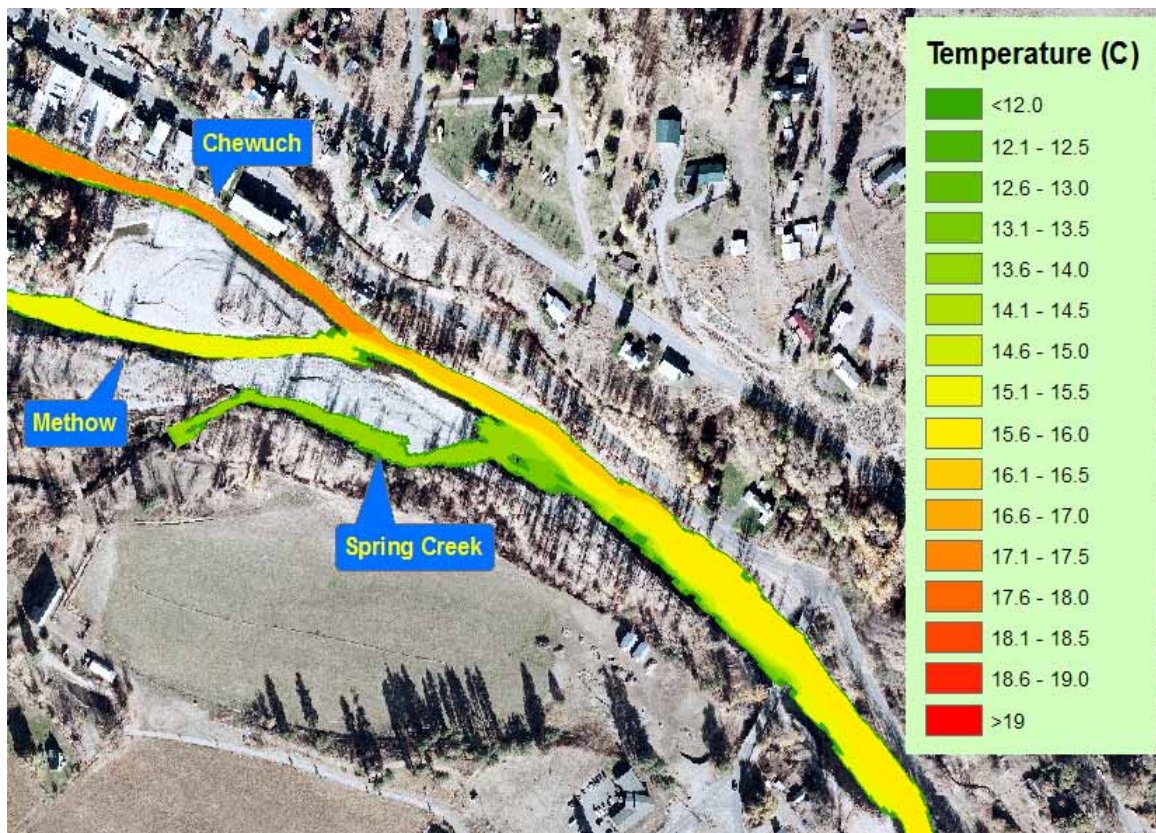


Figure 3-5. SRH-2D numerical simulation of water temperature at the confluences with the Chewuch River and the Spring Creek, modeled with an order of magnitude reduction in the turbulent Prandtl number. Reduction in the turbulent Prandtl number decreases the persistence of temperature gradients downstream of the tributary confluences.

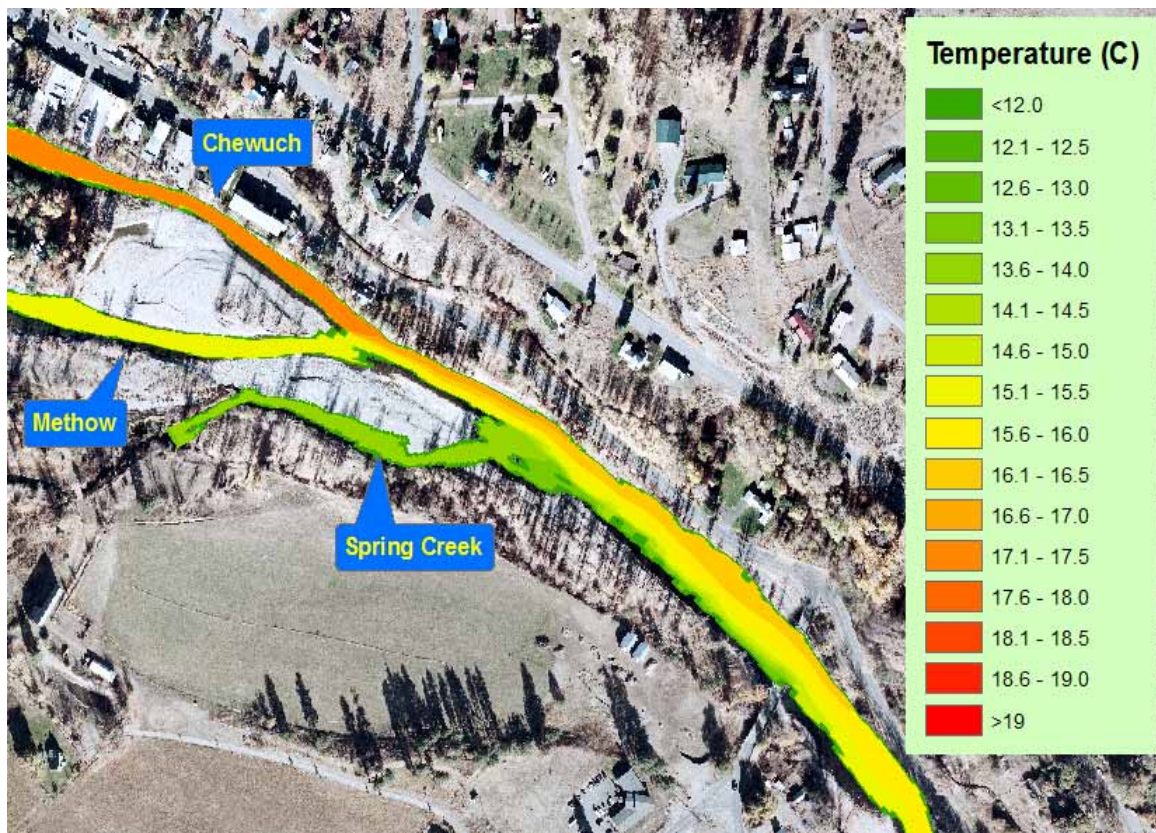


Figure 3-6. SRH-2D numerical simulation of water temperature at the confluences with the Chewuch River and the Spring Creek, modeled with an order of magnitude increase in the turbulent Prandtl number. Increasing the turbulent Prandtl number increases the persistence of temperature gradients downstream of the tributary confluences.

3.2 Test Case with Log Data

In the second test case, SRH-2D is used to simulate unsteady flow and temperature over four months from June 1, 2012 to September 30, 2012. Several temperature loggers in the study reach provided continuous point temperature data that can be used to test model predictions of longitudinal changes in temperature. Three loggers provided continuous temperature measurements for upstream model boundary conditions at flow locations labeled Chewuch Mouth, Methow above Chewuch, and Spring Creek (Figure 3-7 and Table 3-2). Additional temperature logger data is needed to test model predictions along the channel. The logger location labeled Methow at Winthrop provided temperature downstream of the Chewuch and Spring Creek confluence at the US 20 bridge crossing in Winthrop. However, this location is in the temperature mixing zone; data was instead used from the logger located further downstream, labeled Methow above Barkley Diversion. Another logger, Methow below Barkley Diversion, located in the side channel which does not have a surface flow connection with the mainstem Methow River at the time of simulation and could not be used to test the model.

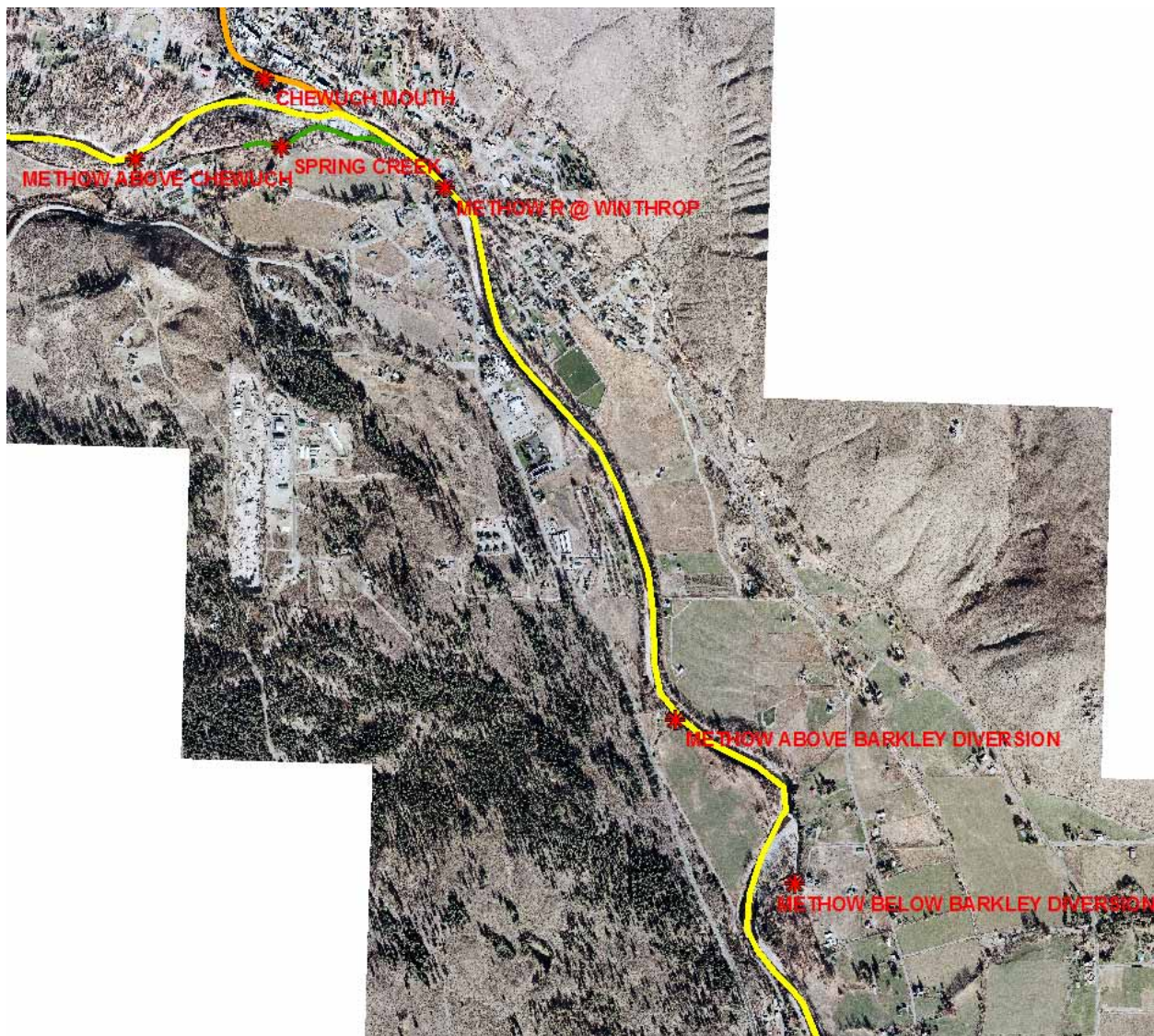


Figure 3-7. Temperature loggers located in the study reach.

Table 3-2 Logger data available in the study reach.

| Logger Location Label | Date Period |
|--------------------------------|--|
| Chewuch Mouth | 6/1/2005 to 9/18/2008, and 7/9/2010 to 10/11/2012 |
| Methow Above Chewuch | 6/30/2005 to 10/15/2009, and 7/16/2010 to 10/16/2012 |
| Spring Creek | 7/2/2005 to 10/15/2009, and 7/16/2010 to 10/16/2012 |
| Methow at Withrop | 6/27/2005 to 10/13/2009 |
| Methow above Barkley Diversion | 11/26/2009 to 10/16/2012 |
| Methow below Barkley Diversion | 11/26/2009 to 10/16/2012 |

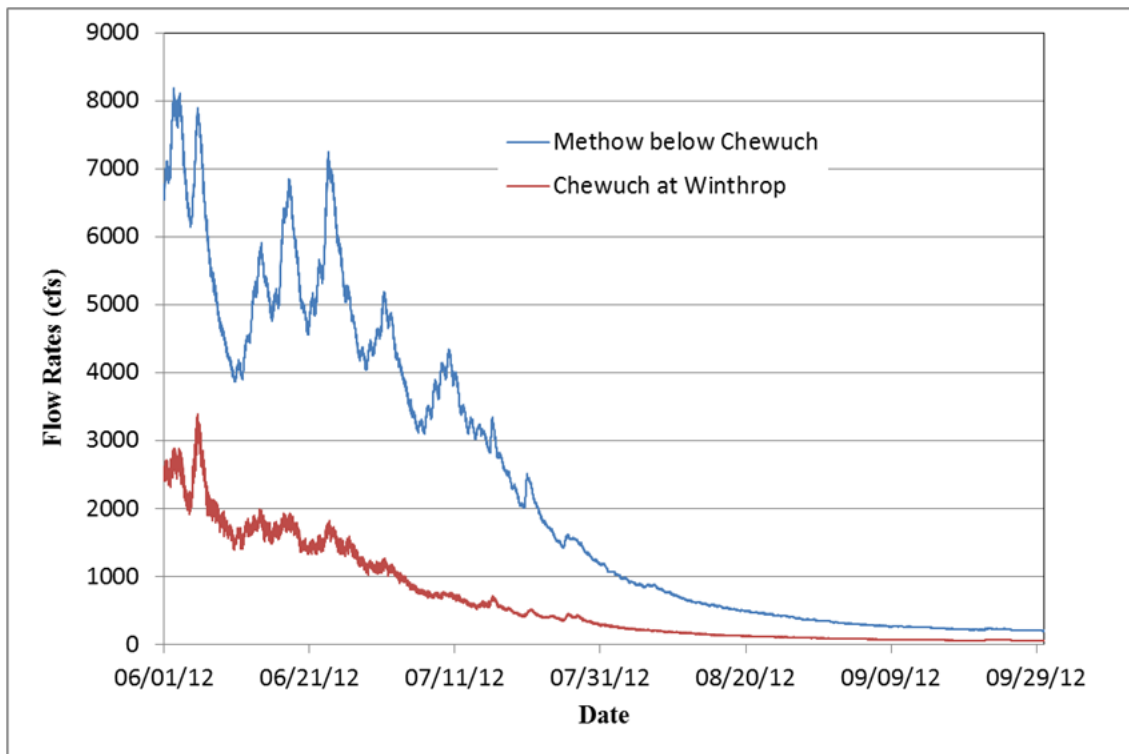


Figure 3-8. Methow and Chewuch hydrographs used as upstream input boundary conditions.

Two gage stations are located in the study reach (Figure 3-8): USGS 12448500 (Methow at Winthrop) and USGS 12448000 (Chewuch at Winthrop). There is no gage to measure flow in Spring Creek. The majority of the contribution from Spring Creek is due to ground seepage and the fish hatchery; further, there is no assumed correlation between the flow rates in the Methow and Spring Creek. For this reason, the same flow distribution used in the first test case was used in the second test case: 20.7cfs from Spring Creek and 20cfs from ground seepage on the right bank. Future field survey is recommended to measure the flow rate in the Spring Creek. The flow rate at the Methow above Chewuch is obtained by substituting the flows at Chewuch and Spring Creek from the downstream gage at Methow at Winthrop.

The longitudinal temperature in the river is affected by the heat gain and loss at the water surface and channel bed. The dominant forms of heat gain are solar (short wave) radiation and atmospheric (long wave) radiation. The dominant forms of heat loss include back radiation from the stream, evaporative heat loss from the stream, and evaporative and conductive heat loss at the water surface. The heat flux to the channel bed is usually positive at day time and negative at night time.

Solar radiation was not directly measured at the study reach, but was estimated from Eqs (2.6) to (2.21) given the cloud covering, elevation, and site latitude and longitude position.

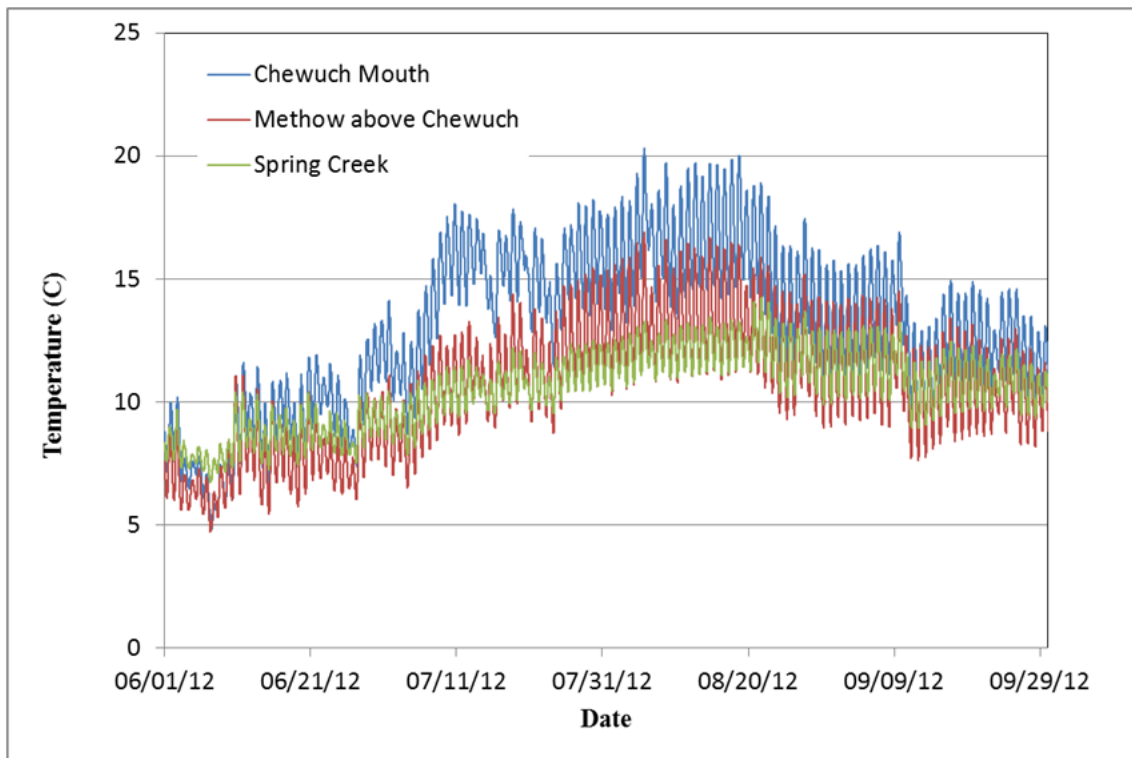


Figure 3-9. Methow, Chewuch, and Spring Creek inflow water temperatures used as upstream input boundary conditions for the model.

Compared with logger data at the Methow above Barkley Diversion location, the model predicted the temperature fairly well (Figure 3-10). The root mean square error is about 0.37°C. No temperature difference was observed in the channel transverse direction (well-mixed) at the Methow above Barkley Diversion location. The wind effect coefficients a_1 and b_1 as defined in Eq. (2.24) were set as 1.0×10^{-9} and 1.0×10^{-9} , respectively. The coefficients were set to their low ends in order to maintain a slightly increased temperature in the downstream direction. To better understand the effects of all source terms, a longer reach is recommended.

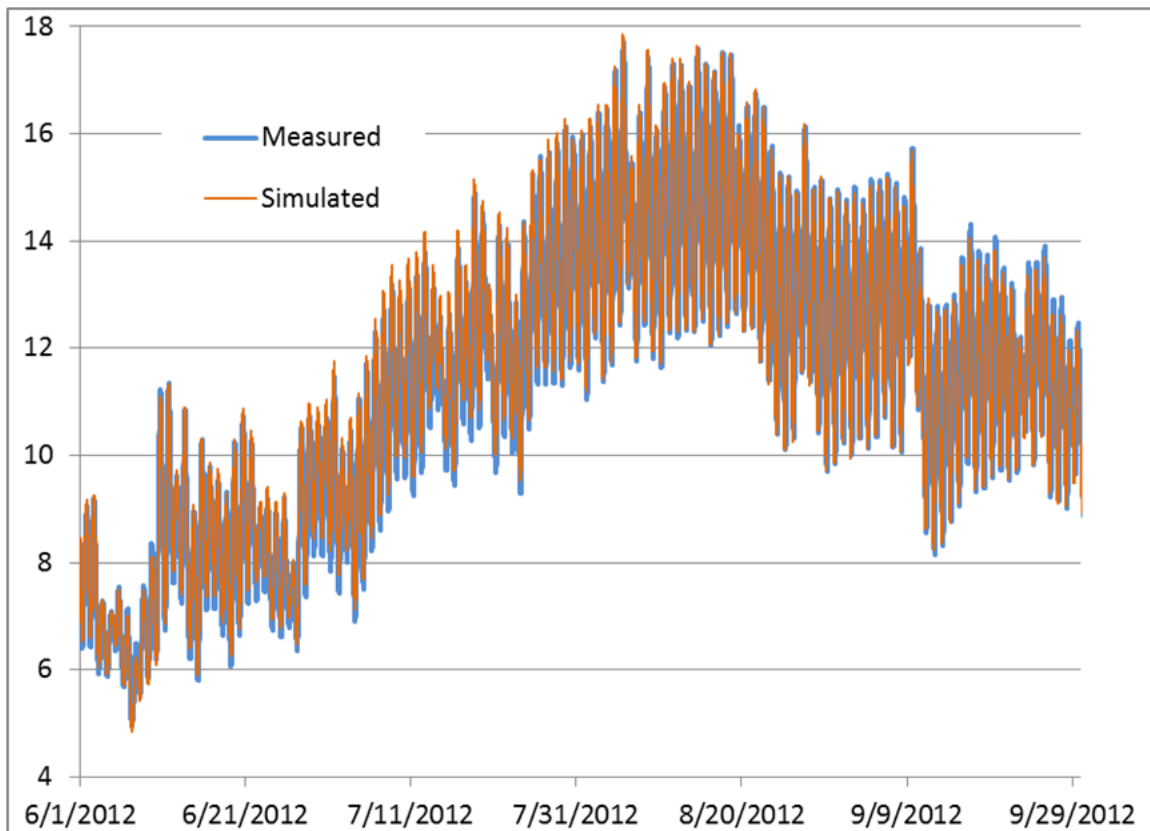


Figure 3-10. Measured and simulated water temperatures at the logger location labeled Methow above Barkley Diversion.

4. Climate Change Impact on the Temperature of the Methow River

SRH-2D was used to study how climate change will alter water temperature in the Methow River. Climate change may increase stream temperature, and the impact may disturb the successful adaptations that salmonids have made to historical temperature patterns in the Pacific West. Higher summer water temperatures may directly affect salmonids in each life stage. It may also affect the fish indirectly through effects on other environmental factors such as food supplies, diseases, dissolved oxygen, and increased predation.

Hourly inputs of meteorology, hydrology, and upstream stream temperatures were taken from the study of Caldwell et al. (2013). The meteorology data includes wind speed (m/s), sky cover (-), air temperature (C), dew point temperature (C), and air pressure (mbar). The solar radiation was calculated directly using equations in section 2.2 given sky cover, dew point temperature, and site parameters. The hydrology data includes flow rates from the upstream Methow River and the upstream Chewuch River. The upstream water temperatures of the Methow River and Chewuch Rivers were used as the upstream boundary condition. It should be noted that there was no information given regarding the flow rates and temperatures from the Spring Creek and ground water inflow just downstream of the Spring Creek, thus the data from year 2009 model calibration was used for future climate change scenarios. Future study on flow and temperature data of the Spring Creek and ground water inflows would provide a more accurate prediction.

Hourly inputs are available for a historical climate simulation, representing 91 years (1 January 1916 to 31 December 2006), and there are 10 GCMs applied in a VIC modeling framework at 3

future periods (a total of 30 sets of input), representative of the years 2020, 2040, and 2080. Additional details on these models and pertinent references may be found in Caldwell et al. (2013).

Currently, it would be impossible to run 91-year length, hourly simulations for the section of the Methow River for 31 (1 historical + 30 future) different sets of hydroclimate conditions. For that reason, subsequent analyses were performed on the individual hourly datasets to select what was considered a range most influential to water temperatures: a hot-dry scenario, a cool-wet scenario, and a median scenario. These three scenarios are available from the historical set and from each set of 10 models for the corresponding future periods of 2020, 2040, and 2080. A single scenario represents a single summer (July 1 – September 30) of hourly data from each set for a total of 12 SRH-2D model input files. Average summer air temperature and average summer flow at the Methow downstream of Chewuch (MDS) site were used to delineate the individual hydroclimate types.

To select the hot-dry scenario, the maximum average temperature and minimum average flow from all available summer vectors (e.g., 91 total for historical and 91*10 for each future period) served as a reference vector. The scaled, Euclidean distances to the reference vector from all other average summer temperature/flow pairs were calculated and the nearest neighbor selected. Similarly, for the cool-wet scenario, the minimum average temperature and maximum average flow were applied as the reference vector. For the median scenario, median values of the average summer temperature and flow were calculated as the reference vector. The scatterplots for the historical and future periods are found in Figure 4-1, with indication of the hot-dry, cool-wet, and median scenarios selected for generation of the hourly time series. Table 4-1 provides additional details on the reference vector, neighbor selected, model selected, and relative year (1916-2016).

Table 4-1. Details of the models picked, reference vectors, and selected values of temperature and flow for each scenario, historical and future period. Relative year indicates the summer within the 1916-2006 sample for each 91-year time series.

| Scenario | Model Selected | Future Period | Ref Temp | Ref Flow | Picked Temp | Picked Flow | Relative Year |
|----------|----------------|---------------|----------|----------|-------------|-------------|---------------|
| Hot-Dry | Historical | Historical | 75.4 | 418.5 | 75.0 | 441.4 | 1979 |
| Cool-Wet | Historical | Historical | 66.2 | 610.4 | 68.0 | 546.3 | 1995 |
| Median | Historical | Historical | 73.4 | 496.1 | 73.5 | 495.3 | 1986 |
| | | | | | | | |
| Hot-Dry | hadgem_1 | 2020 | 76.1 | 410.0 | 75.3 | 480.5 | 1939 |
| Cool-Wet | ccsm3 | 2020 | 61.9 | 1255.9 | 62.5 | 1180.1 | 1954 |
| Median | cnrm_cm3 | 2020 | 69.0 | 525.4 | 68.9 | 528.3 | 1956 |
| | | | | | | | |
| Hot-Dry | ipsl_cm4 | 2040 | 72.3 | 412.5 | 72.3 | 459.4 | 2003 |
| Cool-Wet | cgsm3.1_t47 | 2040 | 62.4 | 1166.5 | 63.9 | 1059.2 | 1935 |
| Median | hadcm | 2040 | 67.2 | 550.8 | 67.1 | 554.4 | 1995 |
| | | | | | | | |
| Hot-Dry | hadgem1 | 2080 | 74.2 | 417.9 | 73.7 | 458.5 | 1958 |
| Cool-Wet | cgcm3.1_t47 | 2080 | 62.7 | 1131.5 | 65.7 | 1098.3 | 1916 |
| Median | cgcm3.1_t47 | 2080 | 69.3 | 511.3 | 69.3 | 503.9 | 2001 |

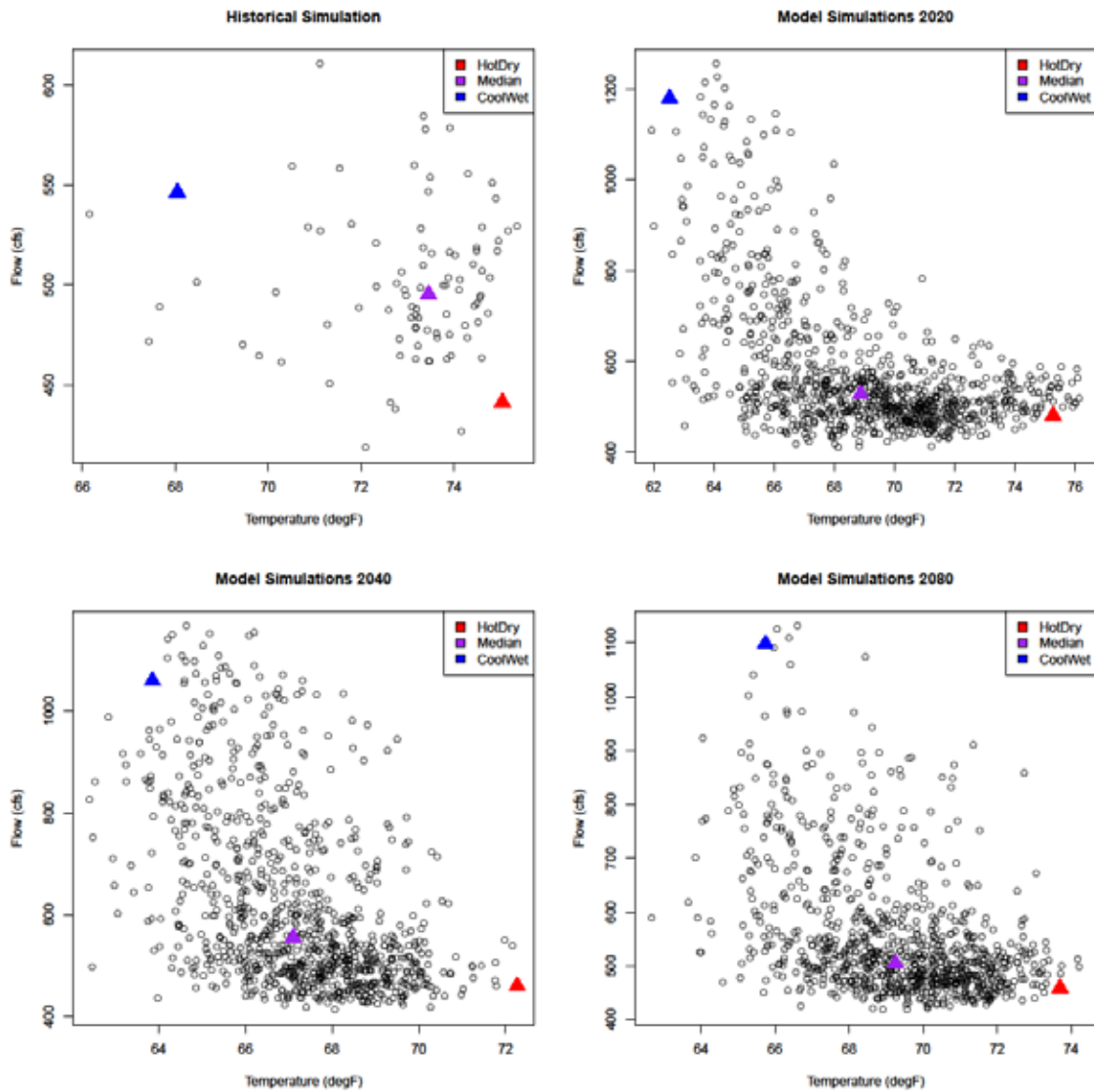


Figure 4-1. Plots of the summer temperature and flow for each historical and future period. Colored triangles indicate the scenario pair selected that is described more fully in Table 4-1. This current study demonstrates how SRH-2D model could be used to predict the water temperature under climate change impact along the rivers where the flow and temperature are only available from simplified VIC simulation and statistical analysis at upstream gage stations. A temperature distribution can be provided by SRH-2D under climate change. Simulated temperatures at the US 20 bridge crossing in Winthrop are presented in Figure 4-2 to Figure 4-4, which could be used to provide information in reaches utilized by endangered or threatened fish species.

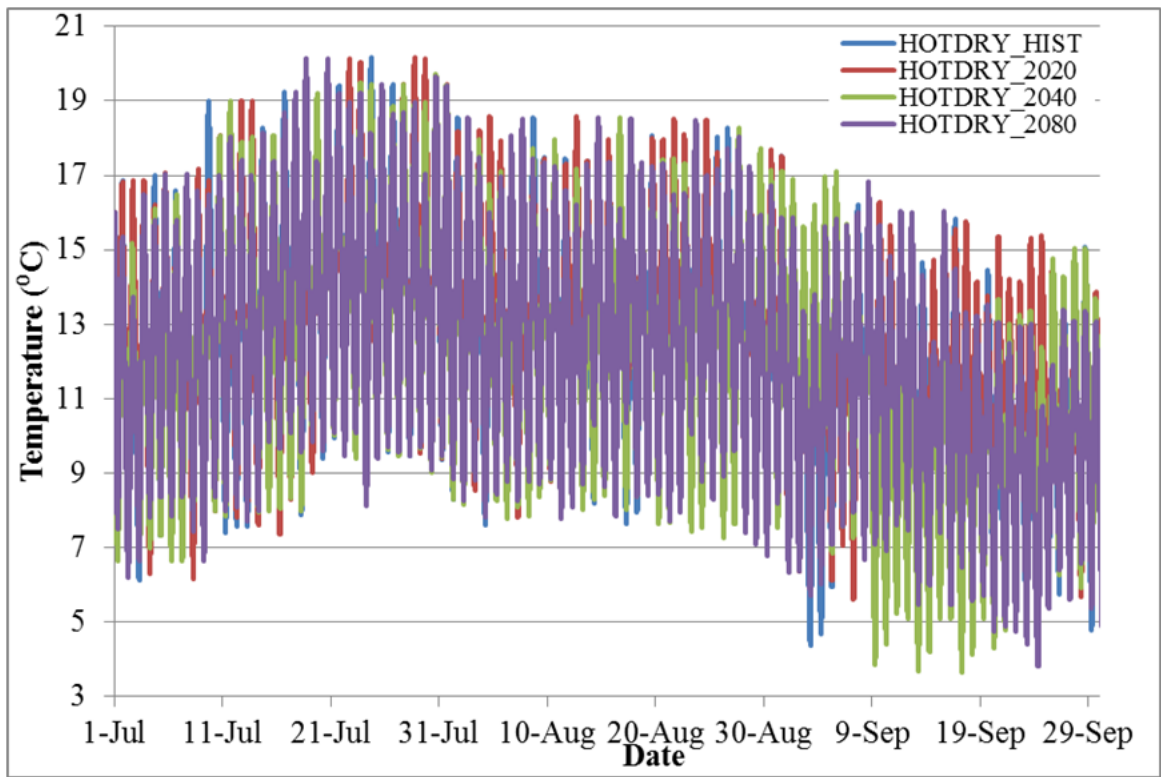


Figure 4-2 Simulated summer water temperature at the US 20 bridge crossing in Winthrop in hot and dry scenario.

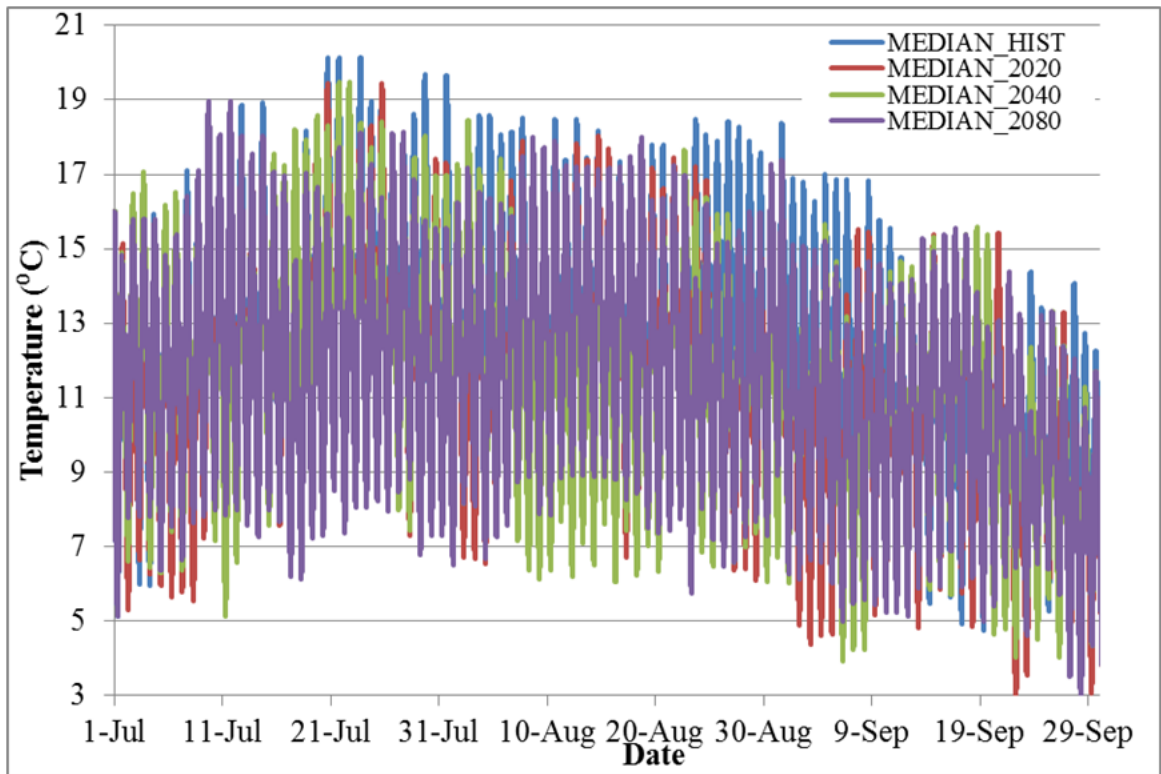


Figure 4-3 Simulated summer water temperature at the US 20 bridge crossing in Winthrop in median scenario.

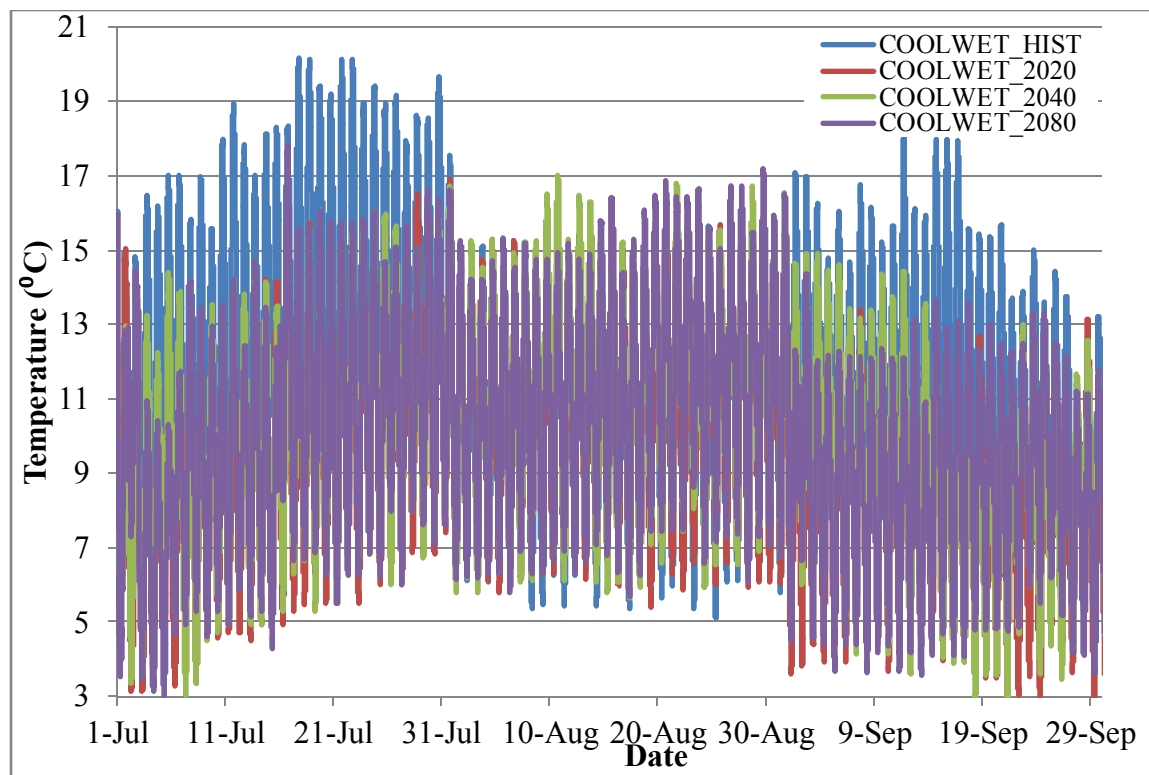


Figure 4-4 Simulated summer water temperature at the US 20 bridge crossing in Winthrop in cool and wet scenario.

To show the impact of the climate change, average summer water temperature at the US 20 bridge crossing in Winthrop for each historical and future period is shown in Figure 4-5. Under the dry-hot scenario, the numerical model predicted an average of 0.2°C temperature increase in 2020, compared with the historical scenario. However, it was predicted the average water temperature would decrease by an average of 0.3 °C and 0.1 °C in 2040 and 2080. The temperature pattern is consistent with the upstream input temperature.

The definition of dry-hot scenario refers to the warmest air temperature-lowest streamflow summer from 910 seasons (i.e., 10 different climate models over a 91-year simulation). It is possible (and evident in this study), that the hot-dry future scenario may have higher streamflow and lower stream temperature during the snow melting season in summer than the historical hot-dry scenario. Researches are recommended to show if there is consist with other data in the Methow River basin. Under cool-wet and median scenario, the water temperatures in 2020 were predicted to be lower than historical and then increases in 2040 and 2080. It is recommended that the dry-hot (water temperature) scenario be used to produce a better prediction regarding the climate change impact on stream temperature in future studies.

It should be noted that the current study of climate change impact on stream temperature is a preliminary demonstration due to several limitations. The major limitation is the scale of the model, which is small (about 4 miles of reach) and the river does not have enough time to absorb the solar and atmosphere radiations and exchange heat with environment. Future large scale model (about 20 miles or longer) requires channel bathymetry and floodplain topography, vegetation coverage, and measured water temperature to better calibrate the numerical model. Currently information is only available in a four mile scale. For future study, predictions are

required regarding flow rates and water temperatures from Spring Creek and from other tributaries (if a larger scaled model is used). A groundwater model is desired for better prediction of groundwater inflow, which is set as a constant in the current model.

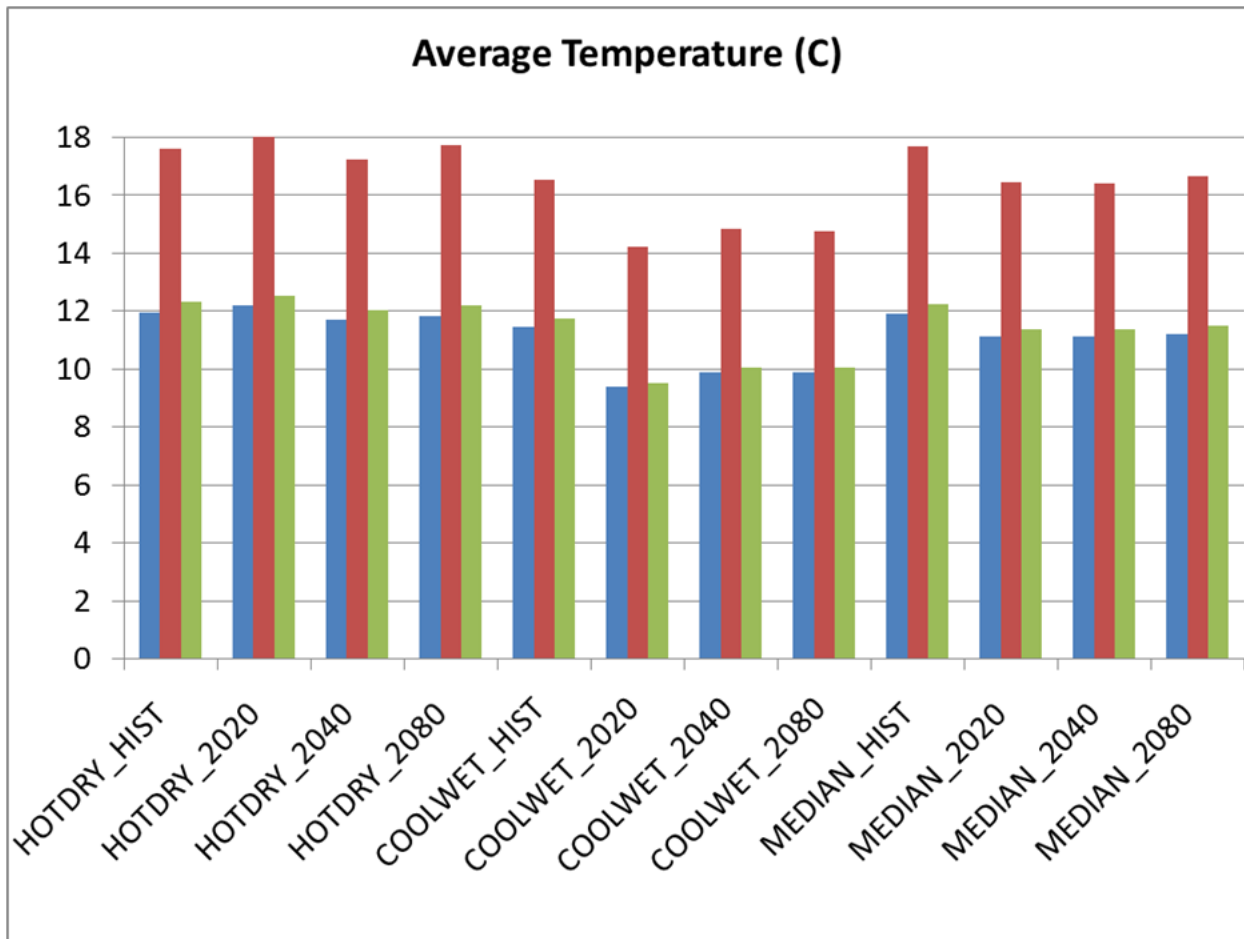


Figure 4-5. Average summer temperature for each historical and future period. Blue represents input temperature at upstream Methow River; red represents input temperature at upstream Chewuch River, and green represents the simulated water temperature at downstream of Methow at Winthrop at the US 20 bridge crossing in Winthrop.

5. Conclusions

Impact of climate change on stream temperature was studied with the SRH-2D temperature model. First, the SRH-2D temperature module was updated and tested using two sets of validation data from the Methow River near Winthrop, WA. Case one calculated a steady-state solution of the lateral temperature mixing zones downstream of the Chewuch (warmer water) and Spring Creek (colder water) confluences without any heat exchange with air and bed. Case two calculated transient solutions of the temperature distribution driven by measured input hydrographs. Then the SRH-2D model was used to study future climate change on stream temperature.

The model showed good accuracy in simulating the lateral temperature mixing zones downstream of tributary confluences when the model is well calibrated by adjusting the turbulent Prandtl number. It was also shown that non-point source boundary conditions may be required to model spatially distributed contributions such as seepage of cold water from a spring.

The model was generally successful in reproducing the measured temporal variation in temperature measured at the Methow above Barkley Diversion location. In this four mile reach, the water temperature is mostly driven by incoming flow discharge and temperature, and not sensitive to weather/climate. For the Methow River, it is hypothesized from measured data that weather impacts to water temperature occur on the scale of multiple reaches, perhaps on the order of tens of river miles.

The climate change impact on the stream temperature was successfully demonstrated in hot-dry, cool-wet, and median scenarios. We found that over a typical river reach of a few miles, the influence of meteorology on water temperature predictions was minimal. Over a reach scale, water temperature predictions were mainly controlled by the incoming water temperature and localized inputs such as the warmer tributary and colder springs. The vast amount of climate change data at an hourly scale posed computational limitations with running the 2D model. We had to reduce the scenarios to a seasonal analysis with representative weather patterns rather than all possible climate change runs.

6. Recommendations

The two-dimensional temperature model is a useful tool for building process-based understanding of thermal dynamics (e.g., sinks, sources, and mixing) in the fluvial environment. The model can be used to help management decisions under climate change impacts manifested through variation in boundary conditions or thermal sources and sinks. The Methow River provided a reasonable test case from which recommendations for further study on computational approaches are made here:

- A longer simulated reach on the order of tens of miles is recommended to better test the stream heat gains and losses, when the temperature increases significantly in the downstream direction. Longer simulated reaches will be required in future studies to demonstrate the effect of climate change on water temperature data.
- Currently the climate change was run under three scenarios: hot-dry, wet-cool, and median. Hotter weather does not usually transform into warmer water temperature. Another scenario should be studied using warm upstream temperature combined with lower discharge.
- Better measurement and integration of groundwater predictions of cold water inflow and temperature will improve local model accuracy within the lateral mixing zones and longitudinal predictions of temperature change.
- Implementation of a groundwater model is recommended to provide more accurate subsurface flow and temperature contributions to supplement measured data and incorporate the ability to do more predictive scenarios.
- A one-dimensional numerical model should be developed to study longitudinal water temperature change for longer reaches and durations where localized two-dimensional flow features are not as relevant.

Acknowledgments

The authors would like to acknowledge the Research and Development Office, Science and Technology Program of the Bureau of Reclamation for providing funding to this research. The authors would like to thank Raymond “Jason” Caldwell, former employee of Bureau of Reclamation, who performed the research on modeling of daily and subdaily stream temperatures which was used as input data in this study. Jason joined the Leonard Rice Engineers, Inc. during the latter stages of this research, however, he continued to provide support and discussions. The authors thank co-workers Yong Lai, Blair Greimann, Dan Dombroski, and Subhrendu Gangopadhyay for discussions and insight. Dan Dombroski’s peer review is appreciated.

References

- Boles, G.L. (1988). *Water Temperature Effects on Chinook salmon (Oncorhynchus Tshawytscha) With Emphasis on the Sacramento River, A literature Review*. State of California, the Resources Agency, Department of Water Resources, Northern District.
- Brekke, L., Pruitt, T., and Smith, D. (2010). *Climate Change and Hydrology Scenarios for Oklahoma Yield Studies*. Water Resources Planning and Operations Support Group, Technical Service Center, Bureau of Reclamation, Denver.
- Brutsaert, W. (1991). *Evaporation into the Atmosphere*. Kluwer Academic Publishers.
- Caissie, D. (2006). "The thermal regime of rivers: A review." *Freshwater*, Vol.51(8), 1389–1406.
- Caldwell, R.J., Gangopadhyay, S., Bountry, J., Lai, Y., and Elsner, M.M. (2013). "Statistical modeling of daily and subdaily stream temperatures: Application to the Methow River Basin, Washington." *Water Resources Research*, Vol.49, 4346–4361, doi:10.1002/wrcr.20353.
- Eagleson, P.S. (1970). *Dynamic Hydrology*. McGraw-Hill, Inc.
- Hauser, G.E., and Schohl, G.A. (2003). *River Modeling System v4 – Vol. 2 Technical Reference*. Report No. WR28-1-590-164, Tennessee Valley Authority, Norris, Tennessee.
- Huber, W.C., and Harleman, D.R.F. (1968). *Laboratory and Analytical Studies of the Thermal Stratification in Reservoirs*. Hydrodynamics Laboratory Technical Report No. 112, Department of Civil Engineering, Massachusetts Institute of Technology, Cambridge, Massachusetts, 277 pp.
- Lai, Yong., and Mooney, D. (2009). "On a Two-Dimensional Temperature Model: Development and Verification." *World Environmental and Water Resources Congress*, 1-14.
- Marciano, J.J., and Harbeck, G.E. (1954). *Mass-transfer studies in Water-loss investigations—Lake Hefner studies*. Technical Report: U.S. Geol. Survey Prof. Paper 269
- Martin, J.L., and McCutcheon, S.C. (1999). *Hydrodynamics and Transport for Water Quality Modeling*. CRC Press.
- Miller, N.L., Bashford, K., and Strem, E. (2003). "Potential Climate Change Impacts on California Hydrology." *Journal of the American Water Resources Association*, Vol.39, 771-784.
- Rodi, W. (1993). *Turbulence models and their application in hydraulics*. 3rd Ed., IAHR Monograph, Balkema, Rotterdam, The Netherlands.
- Tung, C.P., Lee, T.Y., and Yang, Y.C. (2006). "Modeling climate-change impacts on stream temperature of Formosan landlocked salmon habitat." *Hydrological Processes*, Vol.20, 1629-1649.

- Vicuna, S., and Dracup, J.A. (2007). "The evolution of climate change impact studies on hydrology and water resources in California, Climatic Change." *Climatic Change*, Vol.82, 327-350.
- Watershed Sciences. (2009). *Airborne Thermal Infrared Remote Sensing, Methow River Basin, Washington*. Watershed Sciences, Inc, 257B Madison Avenue, Corvallis, OR 97333
- Webb, B.W., Hannah, D.M., Moore, R.D., Brown, L.E., and Nobilis, F. (2008). "Recent advances in stream and river temperature research." *Hydrol. Processes*, Vol.22(7), 902–918.